The 2010 IEEE/RSJ International Conference on
Intelligent Robots and Systems
October 18-22, 2010, Taipei, Taiwan

Implementation of an Automatic Scanning and Detection Algorithm for the Carotid Artery by an Assisted-Robotic Measurement System

Ryu Nakadate, *Student Member, IEEE*, Jorge Solis, *Member, IEEE,* Atsuo Takanishi, *Member, IEEE*, Eiichi Minagawa, Motoaki Sugawara, Kiyomi Niki

Abstract— **In this paper, we present a robotic system which automatically searches and detects the longitudinal section of the carotid artery using a conventional medical ultrasound diagnostic system. In order to obtain a clear image of the carotid artery ready for medical diagnosis, the authors developed real-time image processing algorithms to detect the carotid artery and tissue layers of its walls in the B-mode ultrasound images. Sequential patterns of the ultrasound probe trajectory for scanning the surface of the neck and searching the carotid, were implemented and tested on the Waseda-Tokyo Women's Medical-Aloka Blood Flow Measurement Robot System No. 1 Refined II (WTA-1RII). An experiment with eleven volunteers was carried out and the results show that the system obtained clear images of the carotid artery in 91% of the trials.**

I. Introduction

Heart and vascular diseases are currently among main causes of death in developed countries and even increasing with the aging of the population [1]. Early detection of cardiovascular dysfunction is one of the important techniques in the clinical medicine. For this purpose, in the medical field, the Wave Intensity (WI) is a hemodynamic index that sensitively reflects changes in the state of the circulatory system [2-3]. The WI is usually measured at the common carotid artery (CCA) by an ultrasound diagnostic system and defined by $WI=dP/dt \cdot dU/dt$. Blood pressure (P) is determined by tracking the diameter of the vessel observed in ultrasound image (echo-tracking) and calibrated by the maximum /minimum blood pressure measured by the blood pressure cuff. Blood flow velocity (U) is measured by the Dopplar function of an ultrasound diagnostic system. As the WI function includes the time derivative, consecutive sequences of ultrasound images and real time measurements are required.

Conventionally, the WI measurement is done manually by a sonographer. However, holding an ultrasound probe at the same position for long time is difficult, as the target measurement position is around ±0.5mm from the center of the CCA. There are some passive probe holding devices available in the market, however they are not enough effective. After fixing the passive joint, the probe always slightly moves and the target image is missing. Furthermore, each time the patients move, the operators have to adjust the probe position by releasing and fixing the joints of the probe holder again. That makes overall measurement time longer.

In order to solve this problem, we have developed a carotid blood flow measurement robotic system, the Waseda-Tokyo Women's Medical-Aloka Blood Flow Measurement Robot System No. 1 Refined II (WTA-1RII) [4]. The WTA-1RII is composed of a compact actuated 6-DOFs parallel link manipulator, joystick-type controller and a passive 6-DOFs serial link arm (Fig. 1). In order to perform the measurement with the WTA-1RII, the operator should place the active manipulator close to the patient's neck by moving the passive arm for rough probe-positioning. Then, the joystick controller is used for fine probe-positioning in order to obtain a clear B-mode image of longitudinal section of the CCA. Finally, the operator uses the ultrasound diagnostic system functions to measure the WI. If the patient moves during the above procedure, the operator uses again the joystick to recover the image. Thanks to the support provided by the WTA-1RII, the time required to perform the WI measurement can be reduced [4]. However, in order to provide further support to the operator, we may take advantage of the ultrasound image to provide further feedback to the control system so that we may conceive the implementation of an automated probe positioning. Such a function may enable the operator to concentrate in the measurement itself rather that in the measurement operation of the manipulator. Therefore, in this paper, we focused on proposing and implementing an

Manuscript received March 10, 2010. A part of this research was done at the Humanoid Robotics Institute (HRI), Waseda University. This research was supported in part by Global COE Program "Global Robot Academia", MEXT, Japan. It was also supported by SolidWorks Japan K.K. whom we thank for their financial and technical support.

Ryu Nakadate is with the Graduate School of Advanced Science and Engineering, Waseda University, 2-2 Wakamatsu-cho, Shinjuku-ku, Tokyo 162-8480, Japan (r-nakadate@takanishi.mech.waseda.ac.jp)

Jorge Solis is with the Faculty of Science and Engineering, Waseda University; and a researcher at the Humanoid Robotics Institute (HRI), Waseda University (solis@ieee.org).

Atsuo Takanishi is with the Faculty of Science and Engineering, Waseda University; and one of the core members of the Humanoid Robotics Institute (HRI), Waseda University (contact@takanishi.mech.waseda.ac.jp)

Eiichi Minagawa is with ALOKA Co. Ltd., Japan (http://www2.aloka.co.jp/)

Motoaki Sugawara is with Department of Medical Engineering, Himeji Dokkyo University, Japan

Kiyomi Niki is with the Department of Biomedical Engineering, Tokyo City University, Japan

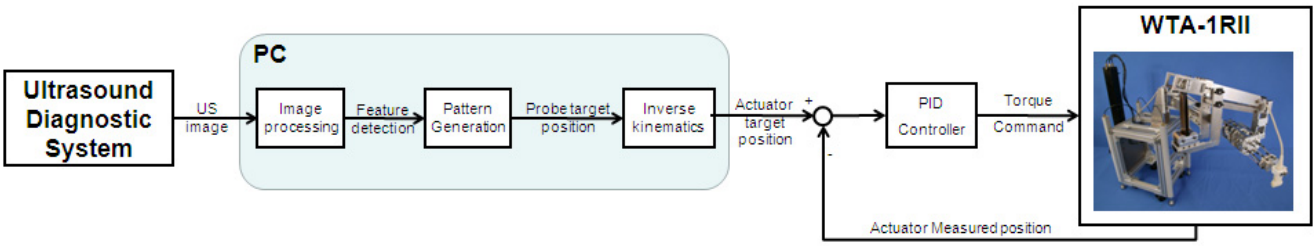

Fig. 1 Block diagram of the proposed automated scanning system designed to automatically detect the carotid artery.

automated probe-positioning algorithm based on the ultrasound image feedback.

Over the last decades, there have been intensive researches on robot-assisted medical ultrasound. The early research which demonstrates the visual servoing using B-mode image feedback is found in [5]. More recently in [6], motion tracking method using speckle information of ultrasound image has been proposed. Such methods basically track the initially existing object in the image frame. However, to the best of our knowledge, there are few researches on automated scanning and detection by means of the robotic system while using the ultrasound diagnostic device. On the other hand, many researches on tele-ultrasound by robotic-assisted platforms mainly use the force control in order to maintain the contact force between skin and probe [7-10]. In our proposed method, no force sensor is required for automated scan but just need image feedback.

In order to detect the CCA during scanning by the robot, in this research, we rather focus on implementing an image processing algorithm to detect, in real-time, the longitudinal section of the CCA by means of the B-mode image feedback. Several researches related to the image processing of the ultrasound data. In particular, some studies have been carried out to detect the CCA and its tissue layers [11-15]. However, most of those proposed ultrasound-image processing algorithms are done off line. In fact, in [11] and [15], it has been reported that the computation time is around 20-24 seconds per frame. For our purpose, it is required to implement a real-time image processing in order to assure the stability of the probe-positioning by means of the WTA-1RII.

II. System Configuration and Requirements

The proposed automated scanning system of the CCA is shown in Fig. 1, which is composed of a medical ultrasound diagnostic system, a probe supporting robot WTA-1RII and a PC for robot control and image processing. In order to compute the probe target position, the output image from the ultrasound diagnostic system is processed and sent it to the pattern generator module, which determines the target trajectory of the probe to adjust its position to find the CCA. By means of the inverse kinematics, the command outputs to all the six motors of the parallel manipulator of the WTA-1RII are generated to assure searching of the CCA.

In order to propose ultrasound image processing algorithms suitable for WI measurement, the following functions are required for the automated searching of the CCA by the WTA-1RII:

1) *Detection of the CCA longitudinal section:* the WI is measured along the longitudinal section of the CCA.
2) *Detection of the intima:* The *intima* (the innermost layer of an artery wall) should be observed. The artery wall consists of three layers, *intima*, *media*, and *adventitia*. The *intima* and *adventitia* are found with higher intensity within the image and the media is shown with lower intensity on the image. The *intima* is clearly observed only when the probe is located at the exact center of the CCA, therefore observation of the *intima* is used as confirmation that the probe is at the right position.
3) *Detection of the contact of the probe with skin*: Initial position of the probe is not always contact with the skin surface.
4) *Keeping the probe contact with the skin during the scan motion*: One of the important tasks of the robotic ultrasound system is maintain the contact of probe with skin to obtain the clear image.
5) *Discrimination of the IJV from the CCA*: the internal jugular vein (IJV) is one of the confounding object and possible to be detected as the CCA. It is difficult to detect from the image processing. However, due to the lower inner pressure of the IJV than the CCA, the IJV can be deformed by outer force. Therefore, once the vessel is found, the probe is moved downwards and the diameter change is observed (Fig. 2).
6) *Keeping guiding the probe towards the target position*: As the exact position where the clearest image is obtained is unknown, the robot should be able to guide the probe towards where clearer image is obtained.

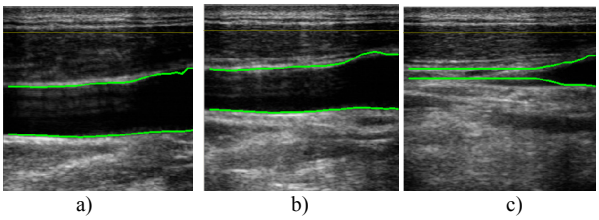

a) b) c)

Fig. 2 Ultrasound image of the IJV: a) without applying pressure, b) with a slight applied pressure by ultrasound probe (3 mm), c) with a higher applied pressure by ultrasound probe (7 mm).

III. Real-Time Detection Method of the CCA

A. Detection of Longitudinal Section of the CCA

The longitudinal section of the CCA is observed as a dark gap (lumen) across the ultrasound image frame bounded by two walls which appear as a high intensity lines. High intensity lines other than artery walls often appear within the image, while the flat dark region is related only to the vessel lumen. Therefore, we have proposed our algorithm to search for the transversal dark gap within the image (Fig. 3).

For this purpose, at first a smoothing filter is applied to reduce the effect of the speckle noise. Then, the grayscale of pixels along the vertical lines (from the top to the bottom of the image) at a regular interval (10 pixels/step) are measured. Possible candidate pixels representing the lumen are labeled by extracting all the dark area which satisfies the below conditions (1). As a result, several short segments of vertical lines are extracted.

$$B=\left\{(x,y):\begin{vmatrix} I(x,y)<T_f(x), \quad T_f(x)=\dfrac{1}{n}\sum_{j=1}^{n}I(x,j) \\ x=10i, i=1,2,...,\dfrac{m}{10} \\ y_1-y_0>\min L, y_0<y<y_1, y_1\neq n \end{vmatrix}\right\} \tag{1}$$

$$\begin{pmatrix} B: set\ of\ extracted\ pixels \\ I(x,y): grayscale\ of\ pixel(x,y),\ 0\le I\le 255 \\ x: horizontal\ axis,\ y: vertical\ axis \\ i: i^{th}\ scanning\ line\ from\ the\ left \\ m,n: \quad size\ of\ image\ frame \\ y_0, y_1: top, bottom\ of\ extracted\ lines \\ minL: threshold\ of\ lengths\ of\ consecutive\ pixels \end{pmatrix}$$

Then, a refined selection among the previous labeled candidates is done. The detected lines are grouped if their bottoms are close to its neighbor. In order to perform the refined selection, we propose a penalty index for evaluating the number of missing lines by using (2).

$$Penalty=\sum_{i=1}^{\frac{m}{10}-1}p_i,\begin{cases} p_i=1: |y_1(i+1)-y_1(i)|\ge gap \\ p_i=0: |y_1(i+1)-y_1(i)|<gap \\ \qquad or\ if\ there is\ no\ y_1(i+1) \end{cases} \tag{2}$$

$$\begin{pmatrix} y_1(i): bottom\ of\ i^{th}\ extracted\ line\ from\ the\ left \\ gap: threshold\ of\ y\ coodinate\ distance\ of \\ \qquad bottom\ point\ from\ neighbor\ extracted\ line \end{pmatrix}$$

The group of the labeled candidates with the minimum penalty index is then chosen. Finally, by applying a smoothing filter for the lines, the CCA walls are therefore extracted.

B. Detection of the Intima

The purpose of detecting the *intima* is a fundamental requirement to guide the probe to exact center of the CCA. Therefore, a precise extraction of the *intima-media-adventitia* interfaces is not required. However, an objective function which evaluates the clearness of the *intima* in the image is required. Due to the tissue layer in the CCA walls, a single wall is observed as double white lines in the B-mode image when the probe is at the exact center of the CCA. Therefore, as a first approach, the proposed algorithm detects the double peaks of grayscale near the CCA walls. However, there are many double peaks in the B-mode image including noise and other tissue. In order to get rid of the effect of them, a small region of interest (ROI) close to the CCA wall is desirable.

For this purpose, after the first detection of the CCA wall, the threshold T_f is increased by one and the processes described in the previous sub-section are re-calculated. Next, the diameter (average distance between near wall and far wall) minus penalty is evaluated. After the iterative process runs for 30 times, the group of maximum evaluation is chosen. As a result, the region of lumen is growing and the contour is detected closer to the walls. The ROI for the detection of the *intima* (next step) is set between several pixels above and below the extracted contour.

After a smoothing filter is applied to reduce the effect of speckle noise, the local maxima of gradient are computed within the ROI. At first, the map of the positive gradient is made (3) by scanning all vertical lines in the ROI from inside towards outside of the CCA. Then, the largest and second largest local maxima of positive gradient in each vertical line are extracted. Within those two pixels, not all, but most of contour of the *adventitia* and the *intima* (if appeared) are included.

$$\begin{aligned} gradient(NW)&=\begin{cases} I(x,y+1)-I(x,y): I(x,y+1)-I(x,y)\ge 0 \\ 0 \qquad\qquad\qquad\quad : I(x,y+1)-I(x,y)<0 \end{cases} \\ gradient(FW)&=\begin{cases} I(x,y-1)-I(x,y): I(x,y-1)-I(x,y)\ge 0 \\ 0 \qquad\qquad\qquad\quad : I(x,y-1)-I(x,y)<0 \end{cases} \\ &(NW=nearwall, FW=farwall) \end{aligned} \tag{3}$$

Finally, the horizontal continuity of candidate pixels is checked. If the *intima* is clearly shown in the image, those two pixels are defined by two smooth lines, otherwise defined by one smooth line and scattered dots. Therefore, a threshold

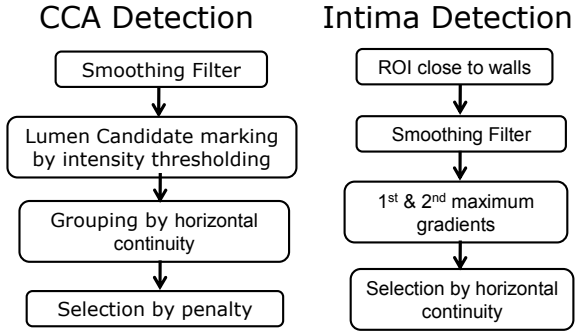

Fig. 3 Flow chart of the proposed image processing algorithm.

of length is applied for the continuity of the extracted pixels. The continuity is defined as follows; if the difference of y-coordinate between two neighbor pixels is zero or one, they are defined as continuous pixels. Only the continuous pixels which length is more than threshold are extracted. The number of extracted pixels is the score of detection of the *intima*.

IV. Probe Path Planning

Before starting automated scanning, the manipulator is set by the operator perpendicularly to the center line of the subject where the probe will be located about 10-20 mm from the approximate CCA location outside center of the neck, then operator clicks start button of the automatic detection sequence. After that, no human intervention is required until the robot system detects the target image which is ready for medical diagnosis. The flow chart of the proposed probe path planning sequence is shown in Fig. 4.

At first, probe is moved downwards until it touches the skin. The detection of contact skin surface is based on calculation of inter-frame differential of grayscale (4); where I is the grayscale of the pixel (x,y) and t is the frame number.

$$D=\sum_{x,y}\{I(x,y,t)-I(x,y,t-1)\} \quad (4)$$

If D is more than threshold, the contact is detected. In order to obtain a clear ultrasound image, the probe surface should keep in contact with the subject's skin. However, the surface of neck is not flat. Sometimes a gap is made between skin and a part of the probe surface. Therefore, if vertical dark zone is detected in the right or left end of ultrasound image, the probe is rotated towards the dark gap in all sequences (Fig. 5a). After first contact with the skin, the probe is moved upward, forward, downward as illustrated in Fig. 5b. The lengths of each arrow *b, c* are 10.0, 7.5mm respectively. The lengths of *d* depend on the shape of the neck. If the lengths of *b, d* are different, it means the probe orientation is not the same as the normal of the neck surface. Therefore the probe is rotated by $e=k(b-d)$, where k is the gain. Although e can be defined by geometrical calculation as $e[\text{rad}]=\tan^{-1}((d-b)/c)$, the measurement of d is not always accurate as the gel on the probe has some thickness, so k should be experimentally determined as smaller value than theoretically calculated.

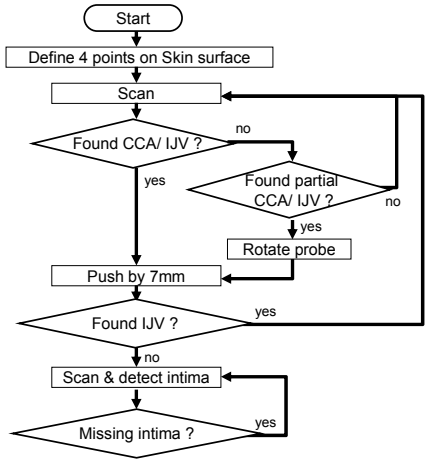

Fig. 4 Flow chart of the proposed probe path planning algorithm.

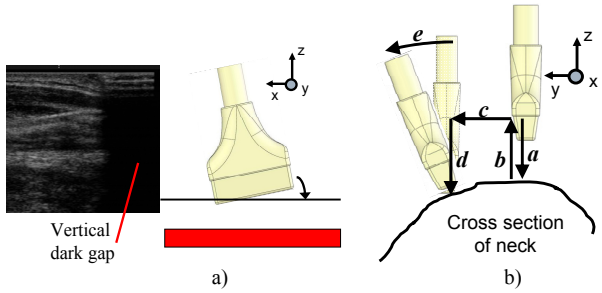

Fig. 5 Probe orientation adjustment a) around y axis by using information from the image detecting vertical dark gap, b) around x axis by using contact information

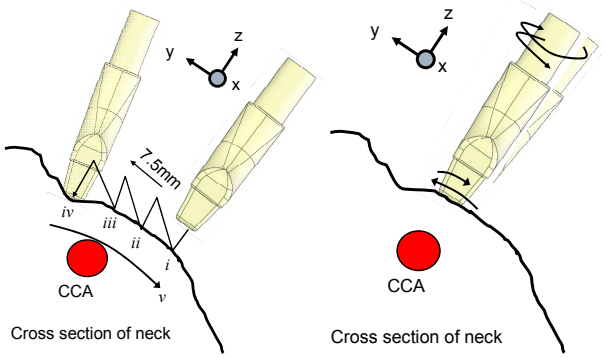

Fig. 6 a) Scanning pattern to search CCA; b) Scanning pattern to search intima

By repeating the above procedure for three times, the manipulator defines four points along the surface of the neck at 7.5 mm regular interval (Fig. 6a). At those four points, the coordinates of six axes are recorded. By interpolating those four points, the scanning path in which the probe can always keep contact with the skin at right angle is obtained.

Then it scans neck surface tracing the path defined the above, and it stops when the probe detects the CCA. In the most case the clear longitudinal section of the CCA appears at first scan. We defined the clear longitudinal section of the CCA as the image which penalty index is less than 20% of image width. However, if the probe and the CCA are not parallel, the observed the CCA in the image will be an ellipsoid dark gap and it is difficult to discriminate from other small dark gaps appearing anywhere. We make use of the motion of the image. The ellipsoid dark gap of the CCA moves across the frame during the scanning while other small dark gaps do not. Therefore, we trace the center of the all of small dark zone in the image and if the width of the locus is more than threshold, we regard it is the partial image of the

CCA.

If the CCA is not detected during the first scan, then the robot repeats the scan with different angle in z axis until the CCA is detected. After detection of the CCA, manipulator moves the probe downwards by 7 mm. If the change on the average diameter is more than threshold, the robot regards the detected objects as the IJV, then the probe will be moved to far side from center of the patient's body and it repeats the CCA searching sequence.

Finally, the purpose of the *intima* searching sequence is to locate the probe where the clearest image of the *intima* is observed. This sequence is done as follows:

1) A small area crossing the CCA is scanned;
2) During scanning, the score of the *intima* is calculated;
3) The maximum score during the above 2) is recorded;
4) When the 80% of the recorded maximum score is reproduced during returning path, the probe stops its movement;
5) Apply the 1)-4) steps for y translational axis and z rotational axis as it is shown in Fig. 6b;

As the maximum score is unknown and the sign of position error is unknown, we have chosen the strategy of "scan and return". Furthermore, there is a hysteresis in the distance of probe and the CCA because of the friction between the probe and the neck skin, therefore returning to the exact recorded position is not effective.

If patient moves during the WI measurement, the suitable image may disappear. So the manipulator is required to recover the probe position. Therefore, if the score of the *intima* is less the 50% of recorded maximum, the manipulator starts the above sequence 1)-5) again.

V. Experiments & Results

The proposed automated scanning algorithms are implemented to the robotic system WTA-1RII. The B-mode image is acquired by 13MHz linear probe of the ultrasound diagnostic system (Pro Sound II SSD-6500SV commercialized by ALOKA Co., Ltd.) at about 20 fps, which outputs the signal in NTSC format, then captured by video grabber Euresys's Picolo Pro 2 into a PC (Pentium 4 3.2GHz). The image processing is implemented by Intel's OpenCV. The captured ultrasound image is 640x480 pixels, and processed region of interest is 322x376 pixels. The PC performs both the image processing and robot control which are written in C++. Including the robot control (sampling time is 5 ms), the frame rate for the image processing was about 14 frames per second.

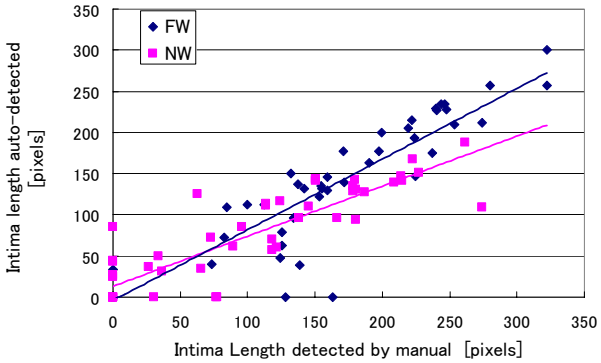

Fig. 7 Experimental results to determine the intima detection rate by the proposed algorithm (FW: far wall; NW: near wall).

A. Image processing algorithm – CCA detection rate

In order to confirm the effectiveness of the proposed CCA detection, we have applied our proposed CCA detection algorithm for 57 images randomly taken from 15 healthy volunteers' (male 13 and female 2). All images contain the longitudinal section of the CCA, while some include ambiguous edges of the CCA walls. In all cases, the CCA detection algorithm has successfully identified the CCA in the images. We evaluated the accuracy of the detected contour of the CCA walls. In this experiment, if the extracted contour is just inside of or on the CCA walls, it is regarded as accurate. On the contrary, if any part of extracted contour is outside of the CCA, the length of such part is measured and divided by whole length of the CCA, and counted as error ratio. The average of error ratio is shown in Table I. There was no error in the far wall (FW) while error ratio of 7% was observed in the near wall (NW). An example of detection error is shown in Fig. 8a. Although the small error does not affect the CCA detection during the scanning sequence, it will affect the *intima* detection rate because the ROI for the *intima* detection is based on the extracted contour of the CCA walls.

B. Image processing algorithm – intima detection rate

The *intima* detection algorithm (including the CCA contour detection process) was applied for the same 57 sample set of the images. The results are shown in Fig. 7; where we can observe the relation between actual length of the *intima* and auto-detected length of the *intima*. Actual lengths were manually measured and confirmed by a skilled doctor. Although they are not in the exact linear relation, the

Table I
The result of CCA detection rate

	Error ratio
NW	7%
FW	0%

Table II
The result of preliminary experiments

	Success	Failed	Total
[cases]	50	5	55
[%]	91%	9%	100%

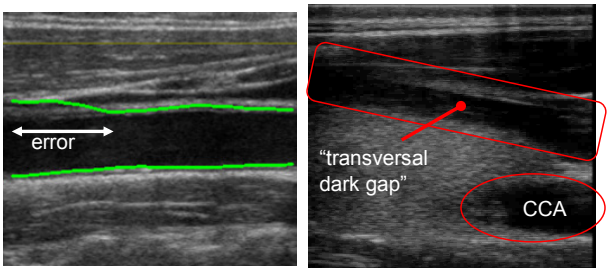

a) b)

Fig. 8 a) Example of the image containing detection error of the CCA walls ; b) Example when the transversal dark gap is appeared (other than CCA or IJV).

result shows enough correlation for guiding ultrasound probe to the direction where the *intima* is clearly observed.

C. Preliminary Experiments

In order to verify the effectiveness of the proposed automated scanning method for the CCA, we have performed an experiment with 11 volunteers (10 males and 1 female, healthy). For this experiment, we have asked the subjects to lay on the bed in supine posture. Then, the manipulator of the WTA-1RII was set perpendicular to the body center line at the position where the ultrasound probe is about 5mm above the neck surface by operator. After that, the operator pushed the start button and waited until whole sequences finish. For each subject, 5 trials have been performed. The video accompanying this paper shows the whole sequence of the scanning. If the robot completed the whole sequence (obtained clear image of the *intima*), the trial was counted as successful. The results are shown in Table II. As we may observe, among total of 55 trials, 50 trials (91%) have been successfully finished. The causes of failed trials are as follows: detected the IJV and could not find the CCA, the transversal dark gap other than vessel appeared (Fig. 8b). In the former case, the robot was trapped a repeat cycle to detect IJV. Further adjustments of system setting such as scanning range in both position and rotation are required. In the latter case, the problem could be easily solved by thresholding the intensity outside the detected contour of the CCA.

VI. Conclusion & Future Work

The algorithms of the robot which automatically searches and detects the CCA and its tissue layers by using medical ultrasound were presented. The effectiveness of the robot system was evaluated by 11 volunteers. Test result was promising.

The proposed algorithm is designed especially considering practical robustness. Although some problems were found in experimental result, they are not difficult to be avoided by implementing some additional algorithms. The more clinical tests are carried out, the more exception might be found. It is the nature of biological measurement. Therefore, this system needs large amount of clinical tests to accumulate the definition what is the CCA and what is not the CCA in the ultrasound image before practical use.

As a future work, the repetitiveness and accuracy of the WI measurement will be compared between manual conventional method and automated method to evaluate the robot system. Then we would like to extend the automated ultrasound diagnosis to the other organs.

References

[1] The World Health Organization, "*The World Health Report 2008 – Primary Health Care*". 2004. pp. 8-9. Available on-line at: http://www.who.int/whr/2008/whr08_en.pdf

[2] A. Harada, T. Okada, M. Sugawara, and K. Niki, "Development of a Non-invasive Real-time Measurement System of Wave Intensity," *in Proc. of IEEE Ultrasonics Symposium*, 2000, pp. 1517-1520.

[3] M. Sugawara, K. Niki, N. Ohte, T. Okada, and A. Harada, "Clinical usefulness of wave intensity analysis," Medical and Biological Engineering and Computing 47:197-206, doi: 10.1007/s11517-008-0388-x..

[4] R. Nakadate, H. Uda, H. Hirano, J. Solis, A. Takanishi, E. Minagawa, M. Sugawara, K. Niki, "Development of Assisted-Robotic System Designed to Measure the Wave Intensity with an Ultrasonic Diagnostic Device," *in Proc. of IEEE/RSJ International Conference on Intelligent Robots and Systems,* 2009, pp. 510-515

[5] P. Abolmaesumi, S. E. Salcudean, W.-H. Zhu, M. R. Sirouspour, and S. P. DiMaio, "Image-Guided Control of a Robot for Medical Ultrasound", *IEEE Trans. on Robotics and Automation*, vol.18, no.1, 2002, pp.11-23.

[6] A. Krupa, G. Fichtinger, G. D. Hager, "Full motion tracking in ultrasound using image speckle information and visual servoing," *in Proc. of IEEE International Conference on Robotics and Automation*, 2007, pp. 2458-2464.

[7] C. Delgorge, et al., "A Tele-Operated Mobile Ultrasound Scanner Using a Light-Weight Robot," *IEEE Trans. on Information Technology in Biomedicine*, vol.9, no.1, 2005, pp. 50-58.

[8] A. Vilchis, J. Troccaz, P. Cinquin, K. Masuda, and F. Pellissier, "A New Robot Architecture for Tele-Echography," *IEEE Trans. on Robotics and Automation*, vol.19, no.5, 2003, pp.922-926.

[9] F. Pierrot, E. Dombre, E. Degoulange, L. Urbain, P. Caron, S. Boudet, J. Gariepy, and J.-L. Megnien, "Hippocrate: a Safe Robot Arm for Medical Applications with Force Feedback," *Medical Image Analysis, Special Issue on Medical Robotics and Computer Assisted Surgery*, vol.3, no. 3, 1999, pp. 285-300.

[10] N. Koizumi, S. Warisawa, M. Nagoshi, H. Hashizume, and M. Mitsuishi, "Construction Methodology for Remote Ultrasound Diagnostic System", *IEEE Trans. on Robotics*, vol.25, no.3, 2009, pp.522-538.

[11] S. Delsanto, F. Molinari, P. Giustetto, W. Liboni, S. Badalamenti, "CULEX-Completely User-independent Layers EXtraction: Ultrasonic Carotid Artery Images Segmentation," in *Proc of IEEE 27th Annual International Conference of the Engineering in Medicine and Biology Society, 2005*, pp.6468-6471

[12] Q. Liang, I. Wendelhag, J. Wikstrand, T. Gustavsson, "A Multiscale Dynamic Programming Procedure for Boundary Detection in Ultrasonic Artery Images," *IEEE Trans. on Medical Imaging*, vol.19, no.2, 2000, pp.127-142

[13] C.Liguori, A. Paolillo, A. Pietrosanto, "An Automatic Measurement System for the Evaluation of Carotid Intima-Media Thickness, " *IEEE Trans. on Instrumentation and Measurement,* vol.50, no.6, 2001, pp.1684-1691

[14] C. P. Loizou, C. S. Pattichis, M. Pantziaris, T. Tyllis, A. Nicolaides, "Snakes based segmentation of the common carotid artery intima media," *Medical & Biological Engineering & Computing*, 2007, vol.45, pp.35–49

[15] F. Destrempes, J. Meunier, M. Giroux, G. Soulez, G. Cloutier, "Segmentation in Ultrasonic B-Mode Images of Healthy Carotid Arteries Using Mixtures of Nakagami Distributions and Stochastic Optimization," *IEEE Trans. on Medical Imaging*, vol.28, no.2, 2009 pp.215-229